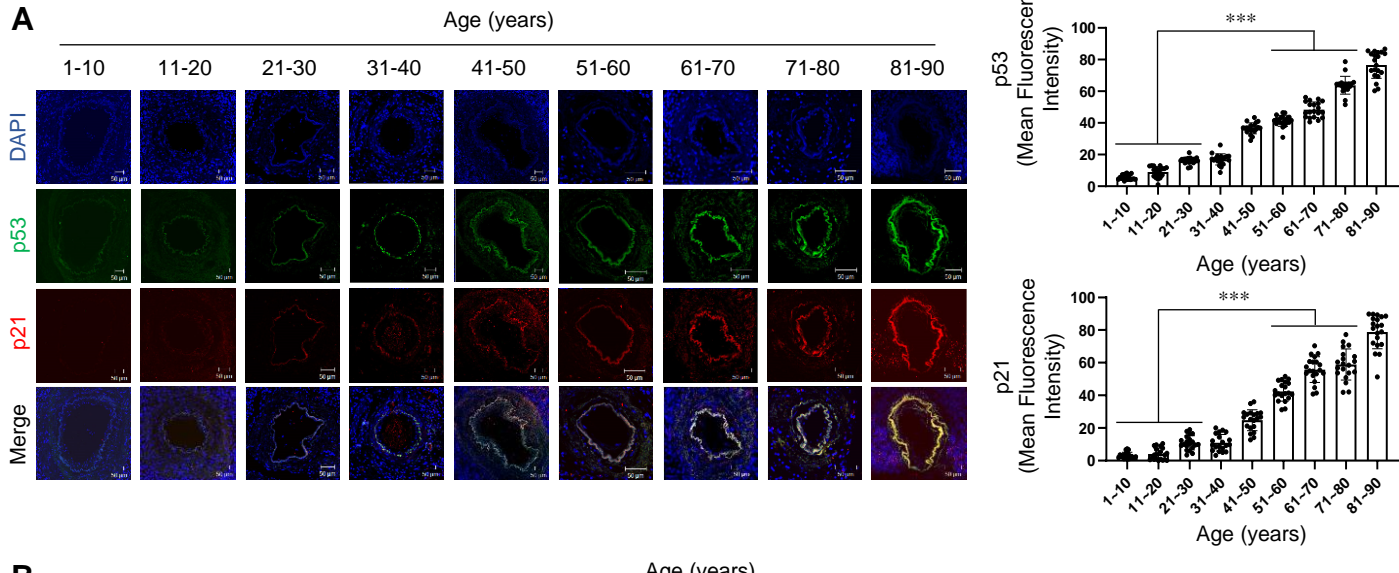
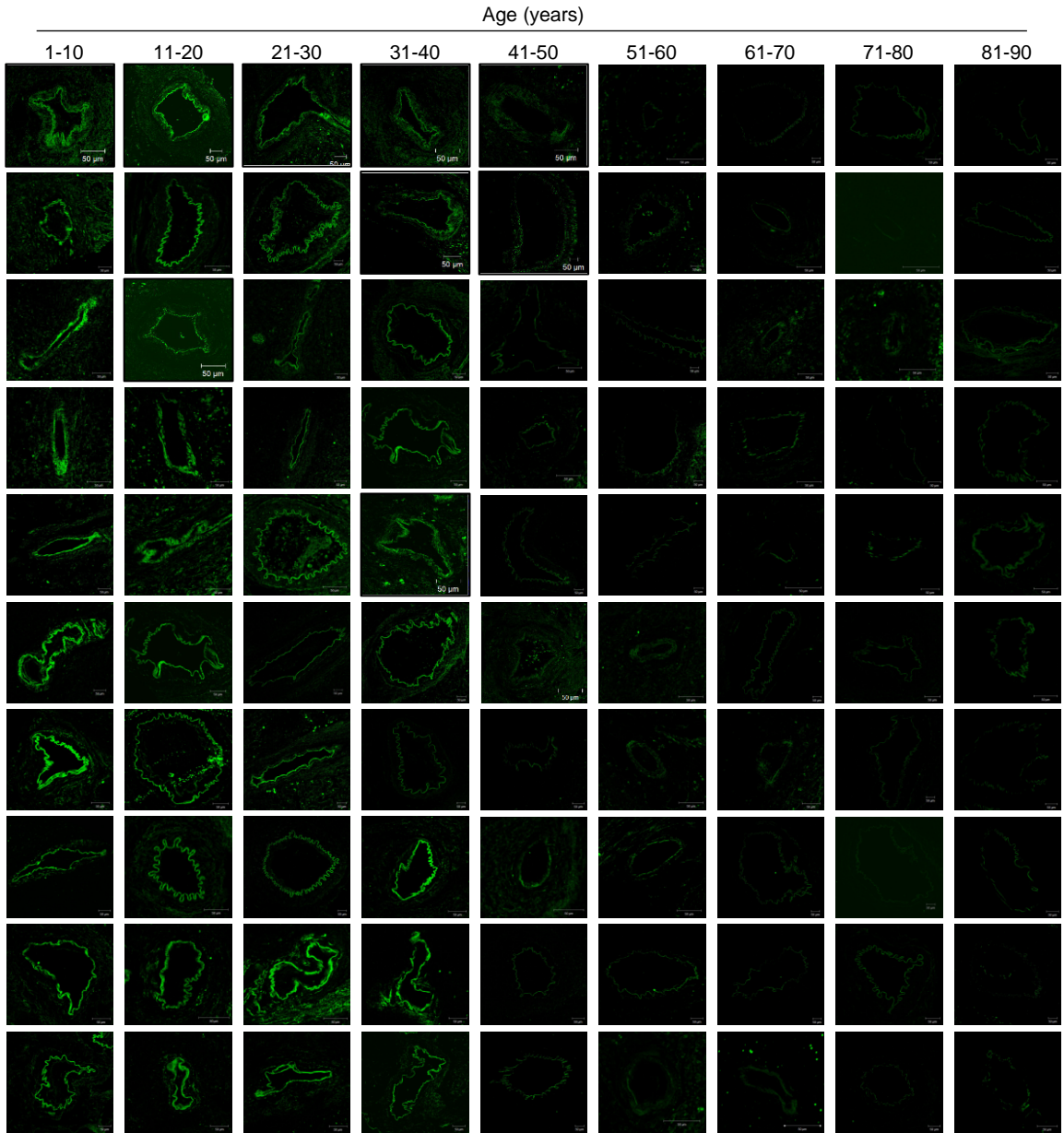


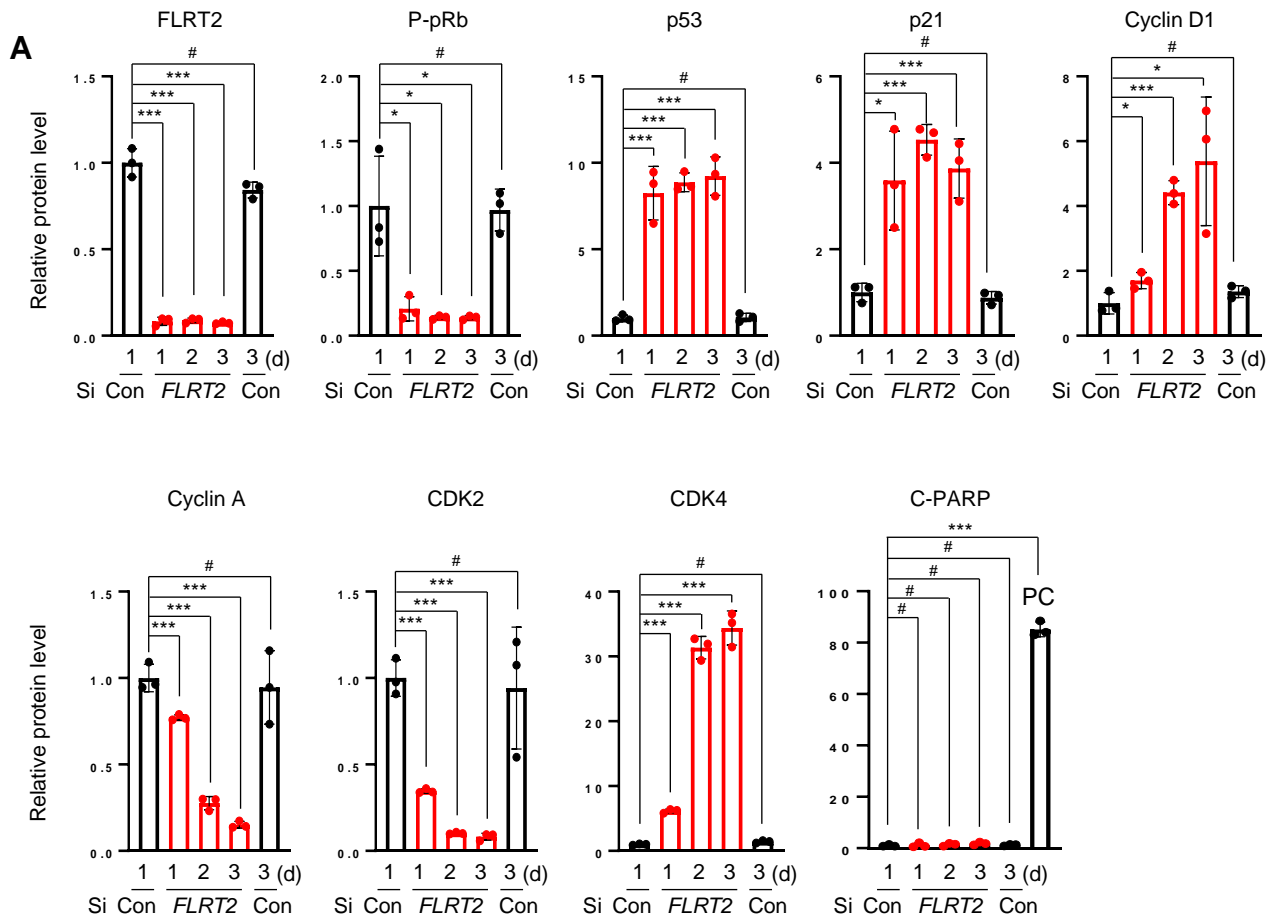
Supplementary Figure 1. Quantitative analysis of immunoblotting data presented in Fig.1A-D

(A-C) The values represent mean \pm SD ($n = 3$; * $P < 0.05$; ** $P < 0.01$). **(D)** The values represent mean \pm SD ($n = 5$; ** $P < 0.01$; *** $P < 0.001$).

A**B**

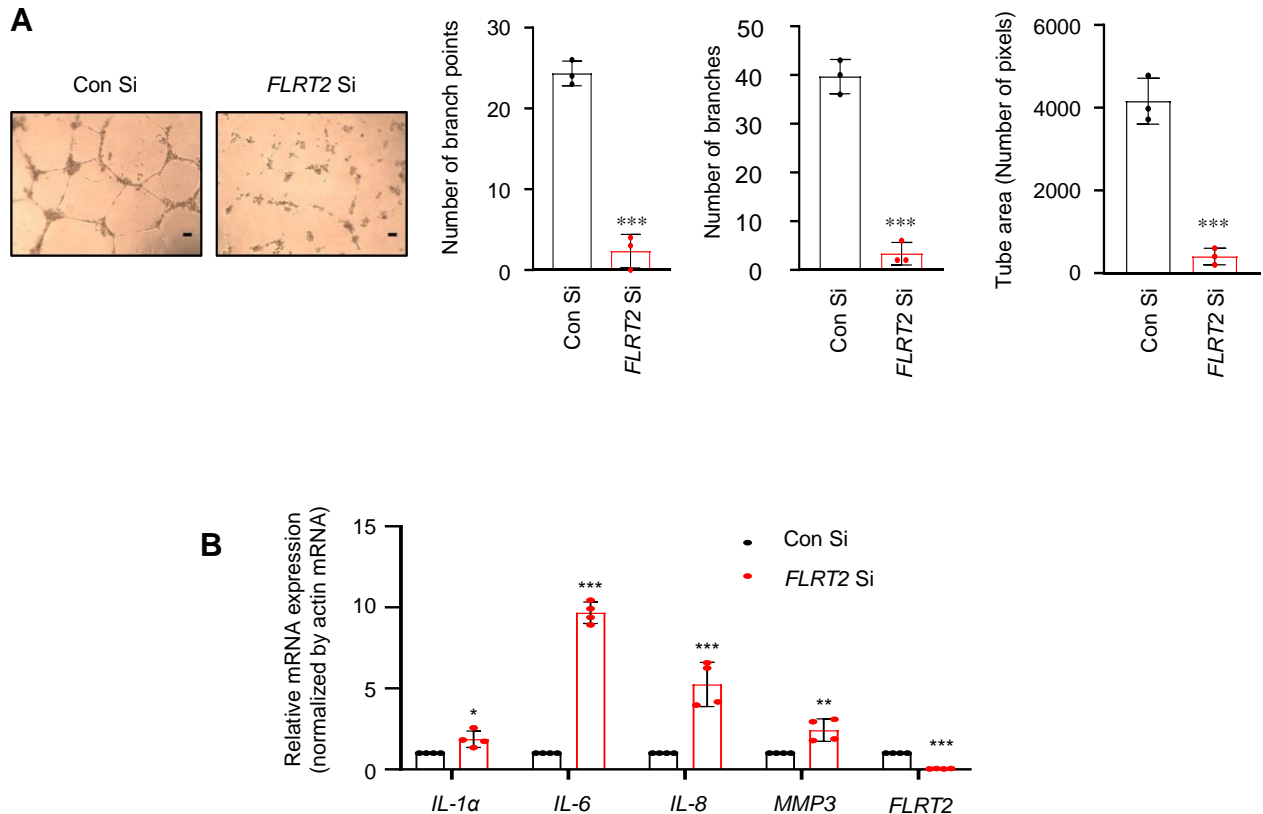
Supplementary Figure 2. Upregulation of p53 and p21, and downregulation of FLRT2 in human arterial tissues with age.

(A) Changes in the expression levels of p53 and p21 in human arterial tissues of each age group were detected using immunofluorescence. Scale bar: 50 μ m. The values represent mean \pm SD (each, n = 20; ***P < 0.001). **(B)** Representative immunohistochemical images of human arterial tissues with age for FLRT2 (each, n = 10). Scale bar: 50 μ m.



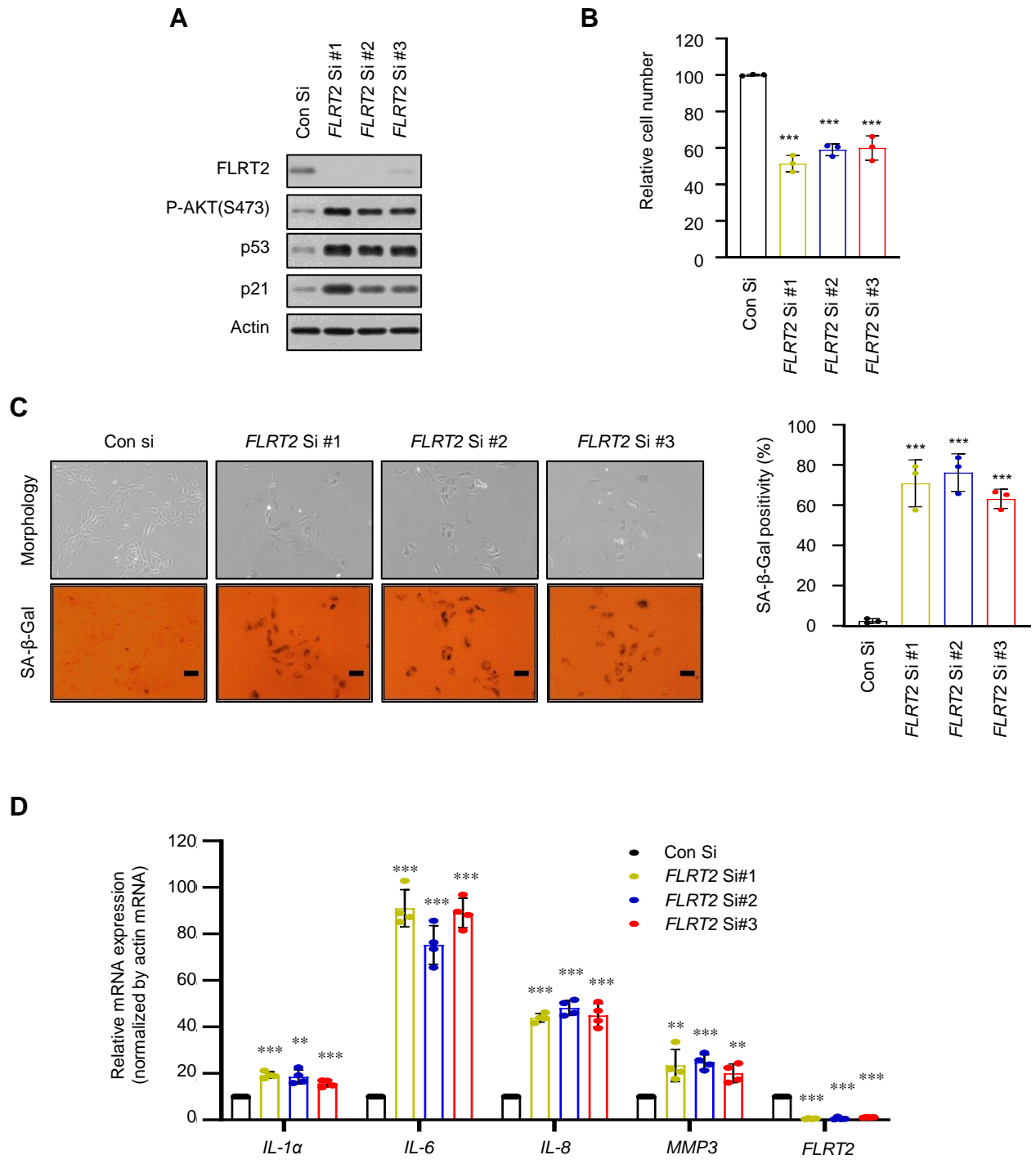
Supplementary Figure 3. Quantitative analysis of immunoblotting data presented in Fig. 2B

(A) The values represent mean \pm SD ($n = 3$; #P > 0.05; *P < 0.05; ***P < 0.001).



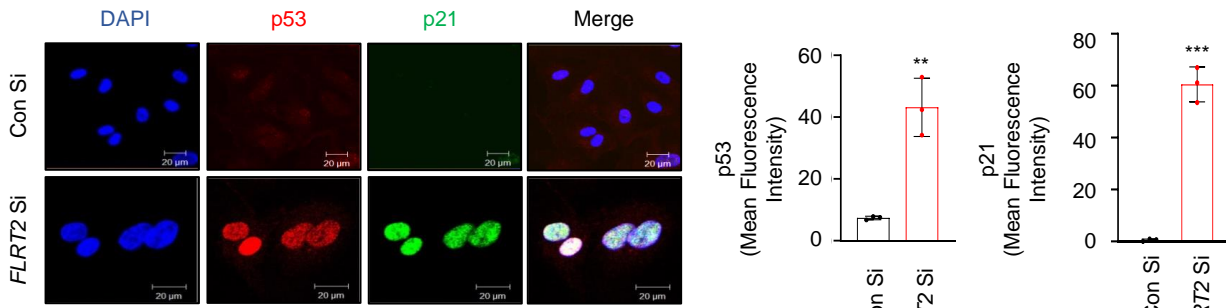
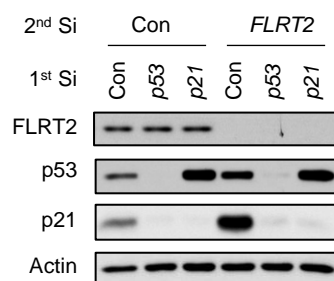
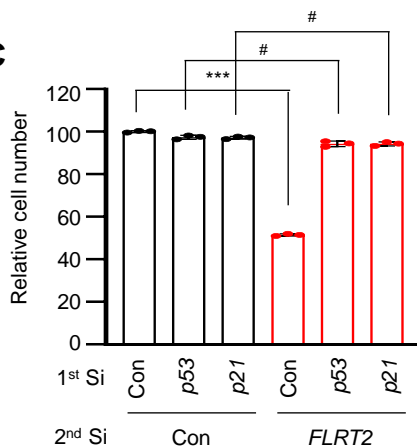
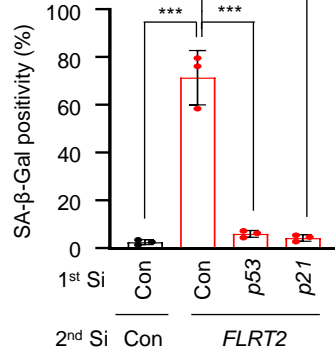
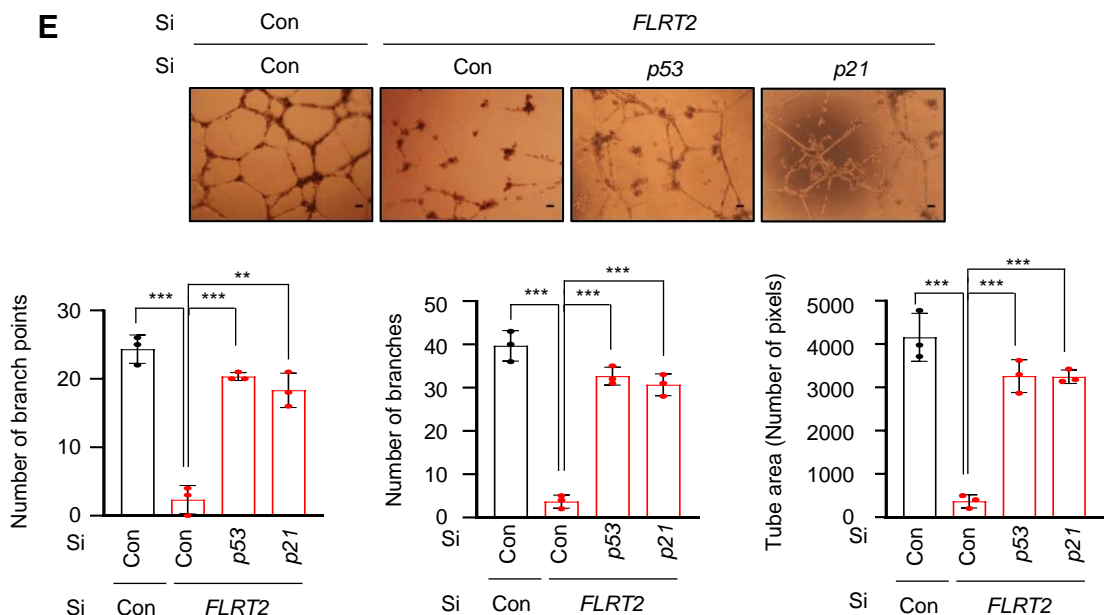
Supplementary Figure 4. *FLRT2* depletion induces decrease of tube formation ability and increase of expression levels of SASP factors.

(A) Tube formation ability of siRNA-transfected HUVECs was analyzed using the endothelial cell tube formation assay. Scale bar: 100 μ m. **(B)** Relative mRNA expression levels of genes related to the senescence-associated secretory phenotype (SASP) in the siRNA-transfected HUVECs were examined using quantitative real-time polymerase chain reaction (qRT-PCR). The values represent mean \pm SD ($n = 3$; # $P > 0.05$; * $P < 0.05$; ** $P < 0.01$; *** $P < 0.001$).



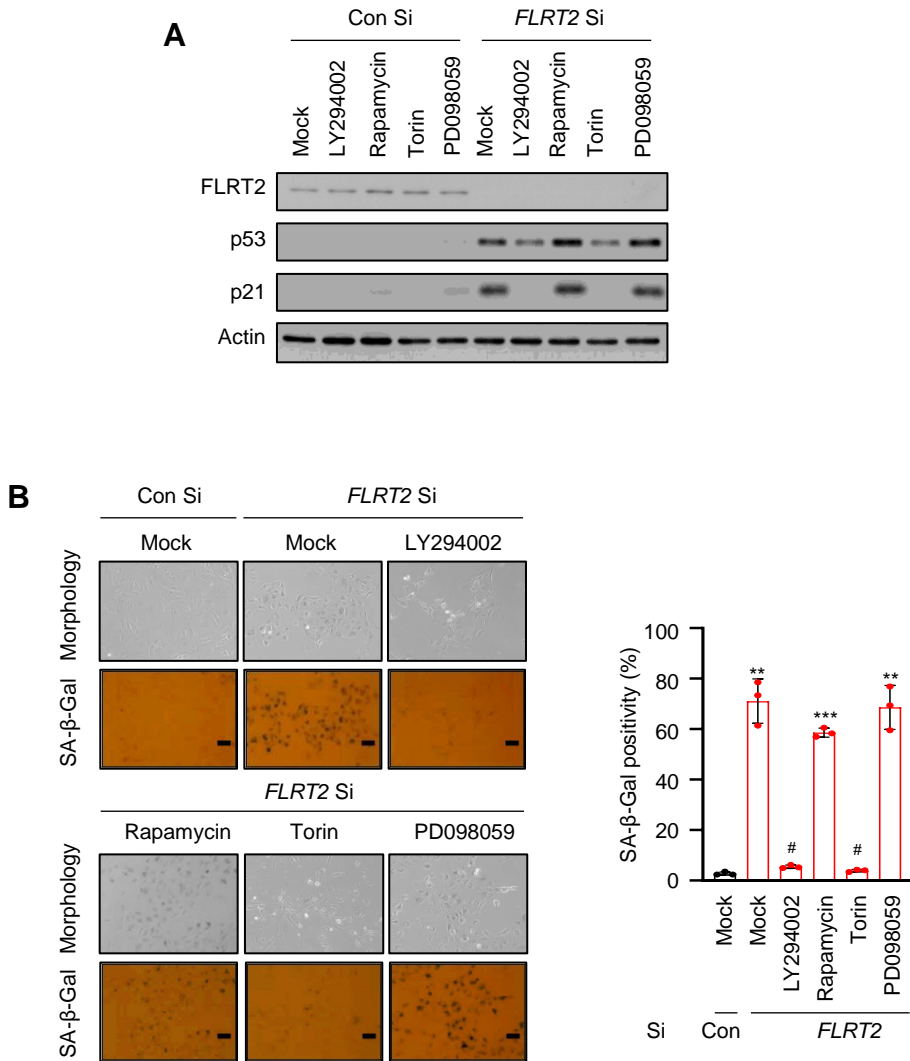
Supplementary Figure 5. No off-target effects of *FLRT2* siRNAs on endothelial cell senescence.

(A-D) HUVECs were transfected with the indicated siRNAs. **(A)**, Immunoblot assay was performed at day 2 post-transfection. **(B)**, Relative cell number, **(C)** SA- β -Gal activity, and **(D)** quantitative real-time polymerase chain reaction (qRT-PCR) analyses were performed at day 3 post-transfection. Scale bar: 10 μ m. The values represent mean \pm SD ($n = 3$; **P < 0.01; ***P < 0.001).

A**B****C****D****E**

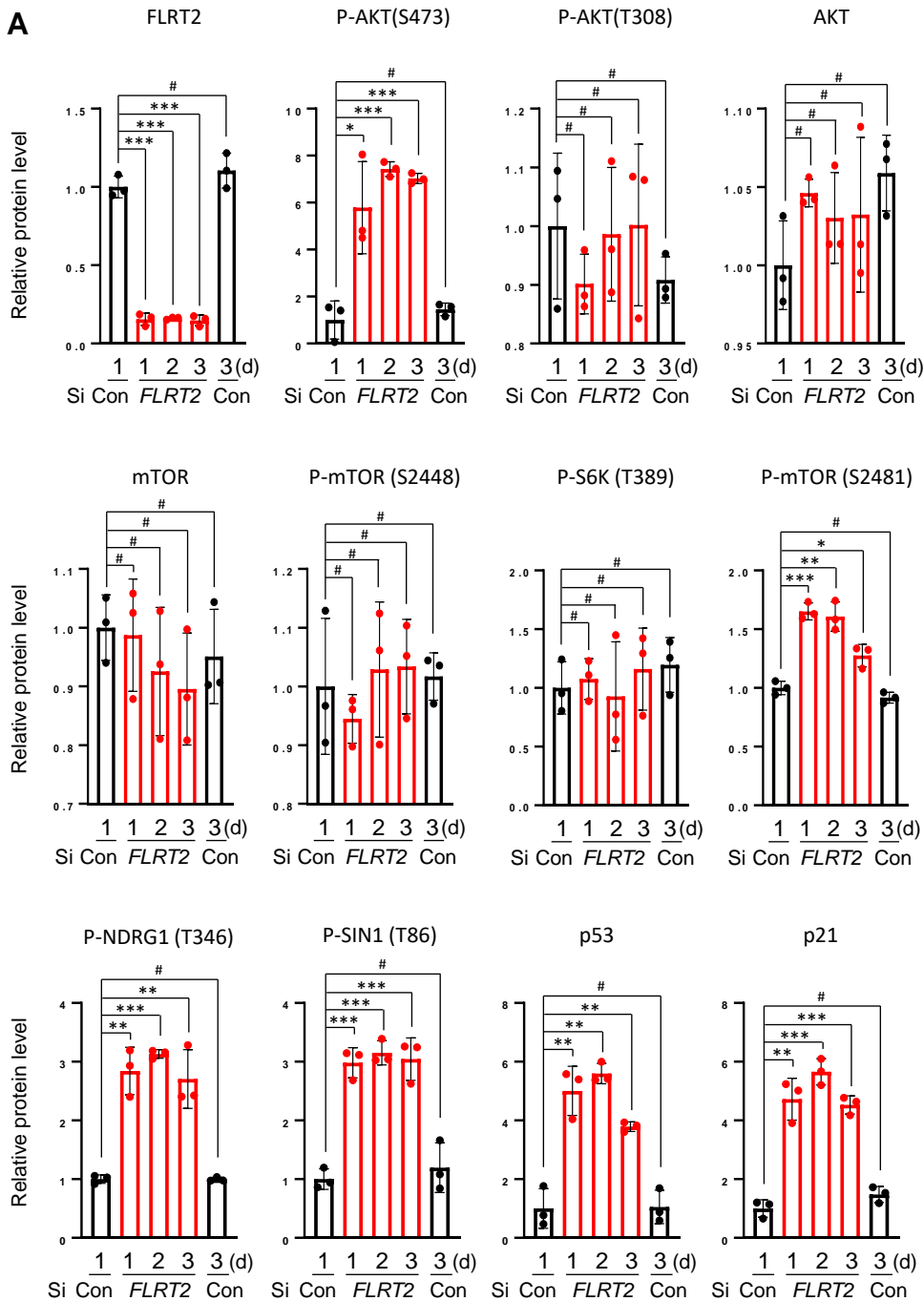
Supplementary Figure 6. *FLRT2* depletion-induced endothelial cell senescence is mediated by the p53-p21 signaling pathway.

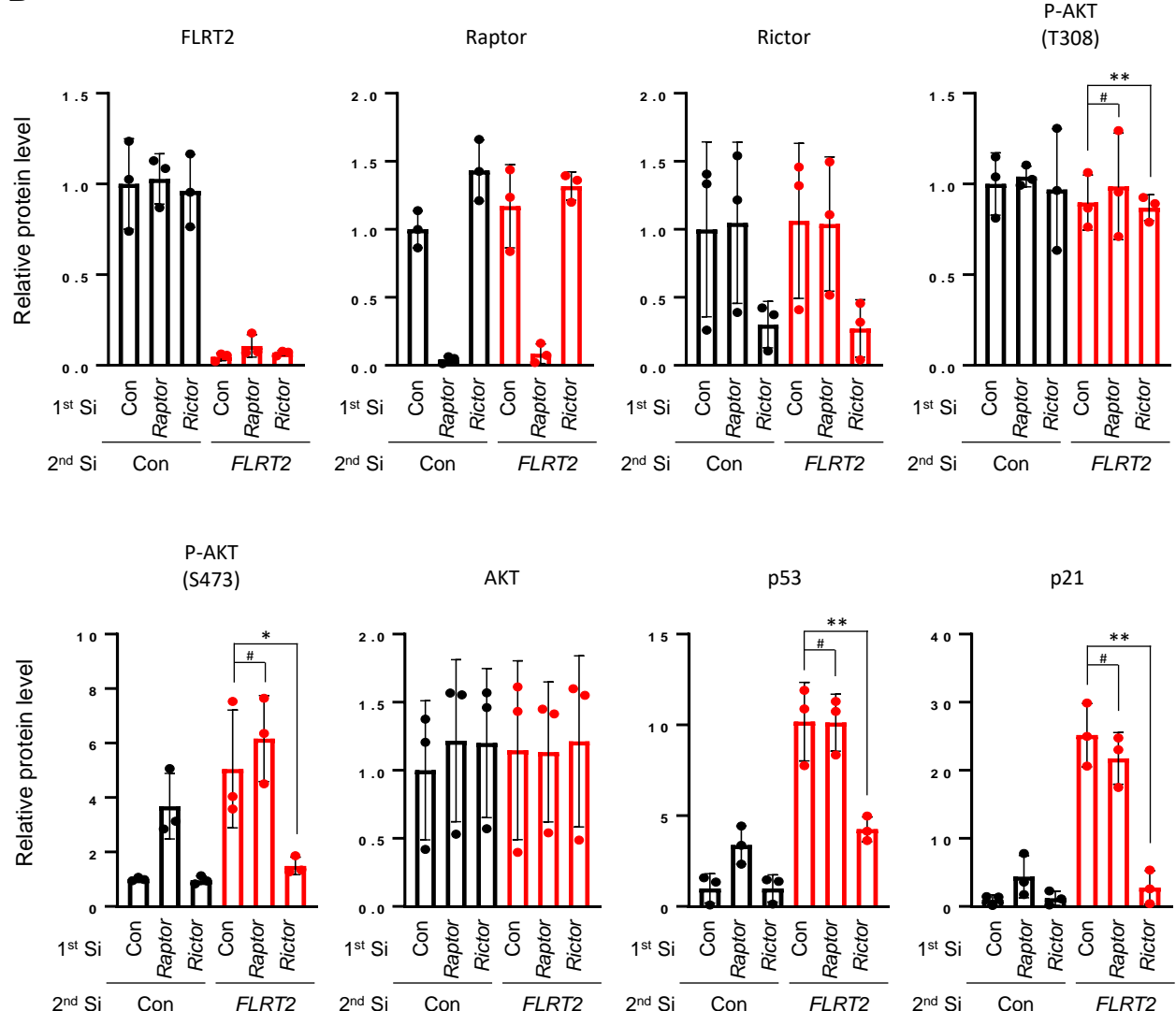
(A) HUVECs were transfected with Con Si or *FLRT2* Si. At day 2 post-transfection, the expression levels of p53 and p21 were examined using immunofluorescence. Quantitative data are shown in the graph. **(B-E)** HUVECs were transfected with Con Si, *p53* Si, or *p21* Si at 6 h before transfection with Con Si or *FLRT2* Si. At day 2 post-transfection, the cells were harvested and subjected to immunoblot assays **(B)**. Relative cell number **(C)**, SA-β-gal activity **(D)**, and endothelial cell tube formation **(E)** were analyzed at day 3 post-transfection. Scale bar: 100 µm. The values represent mean ± SD ($n = 3$; #P > 0.05; **P < 0.01; ***P < 0.001).

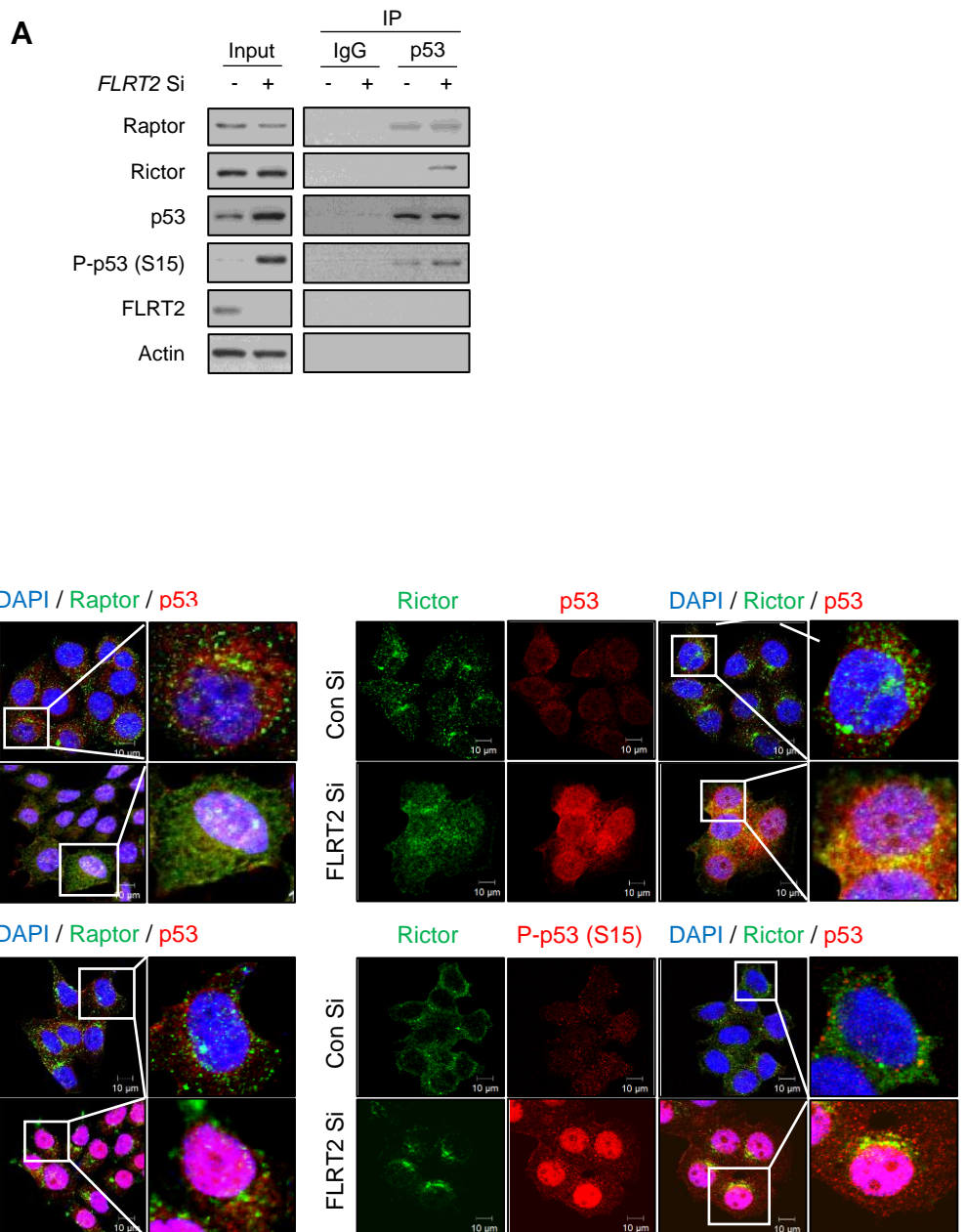


Supplementary Figure 7. Inhibitors of PI3K and mTORC affect *FLRT2* depletion-mediated endothelial cell senescence.

(A, B) HUVECs were transfected with Con Si or *FLRT2* Si for 24 h and treated with the indicated inhibitors. LY294002, rapamycin, Torin, and PD098059 inhibit PI3K, mTORC1, mTORC1/2, and ERK, respectively. Immunoblot assay was performed at 6 h post-transfection **(A)**. At day 3 post-transfection, SA- β -Gal activity was assessed, and the percentage of senescent cells was quantified. Scale bar: 10 μ m **(B)**. **(C-D)** Quantitative analysis of immunoblotting data presented in Fig. 2F-G. The values represent mean \pm SD ($n = 3$; # $P > 0.05$; * $P < 0.05$; ** $P < 0.01$; *** $P < 0.001$). **(E)** HUVECs were transfected with Con Si or *FLRT2* Si. At day 2 post-transfection, cells were fixed and stained with anti-Raptor, anti-Rictor, anti-p53, and anti-p53 (S15) antibodies after permeabilized with Triton X-100. Scale bar, 10 μ m. **(F)** HUVECs were transfected with Con Si or *FLRT2* Si. At day 2 post-transfection, cell lysates were subjected to IP with anti-p53 antibody, and performed immunoblot assays with the indicated antibodies.

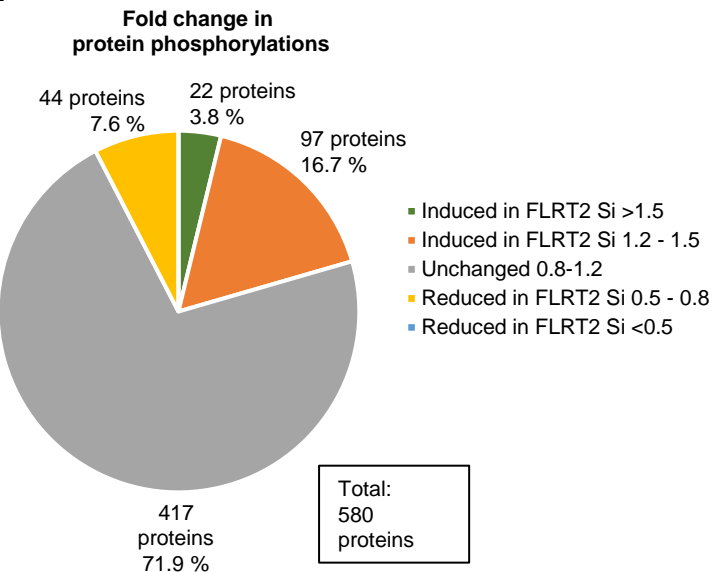
A**Supplementary Figure 8. Continued**

B**Supplementary Figure 8. Quantitative analysis of immunoblotting data presented in Fig. 2F-G****(A-B)** The values represent mean \pm SD ($n = 3$; # $P > 0.05$; * $P < 0.05$; ** $P < 0.01$; *** $P < 0.001$).

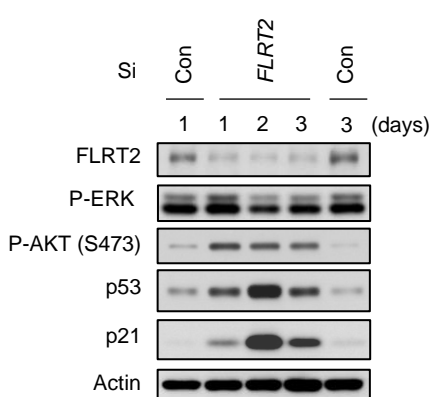
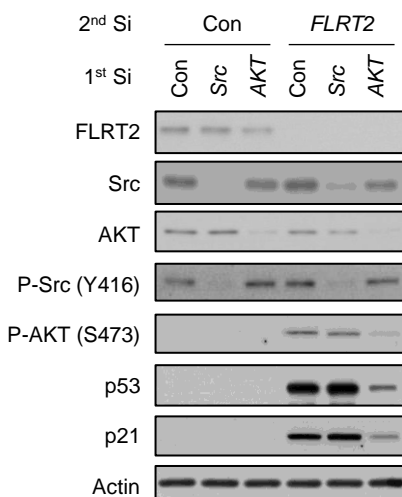


Supplementary Figure 9. Localization of Raptor, Rictor, and p53 in FLRT2-depleted HUVECs.

(A) HUVECs were transfected with Con Si or FLRT2 Si. At day 2 post-transfection, cell lysates were subjected to IP with anti-p53 antibody and performed immunoblot assays with the indicated antibodies. **(B)** HUVECs were transfected with Con Si or FLRT2 Si. At day 2 post-transfection, cells were fixed and stained with anti-Raptor, anti-Rictor, anti-p53, and anti-p53 (S15) antibodies after permeabilized with Triton X-100. Scale bar, 10 µm.

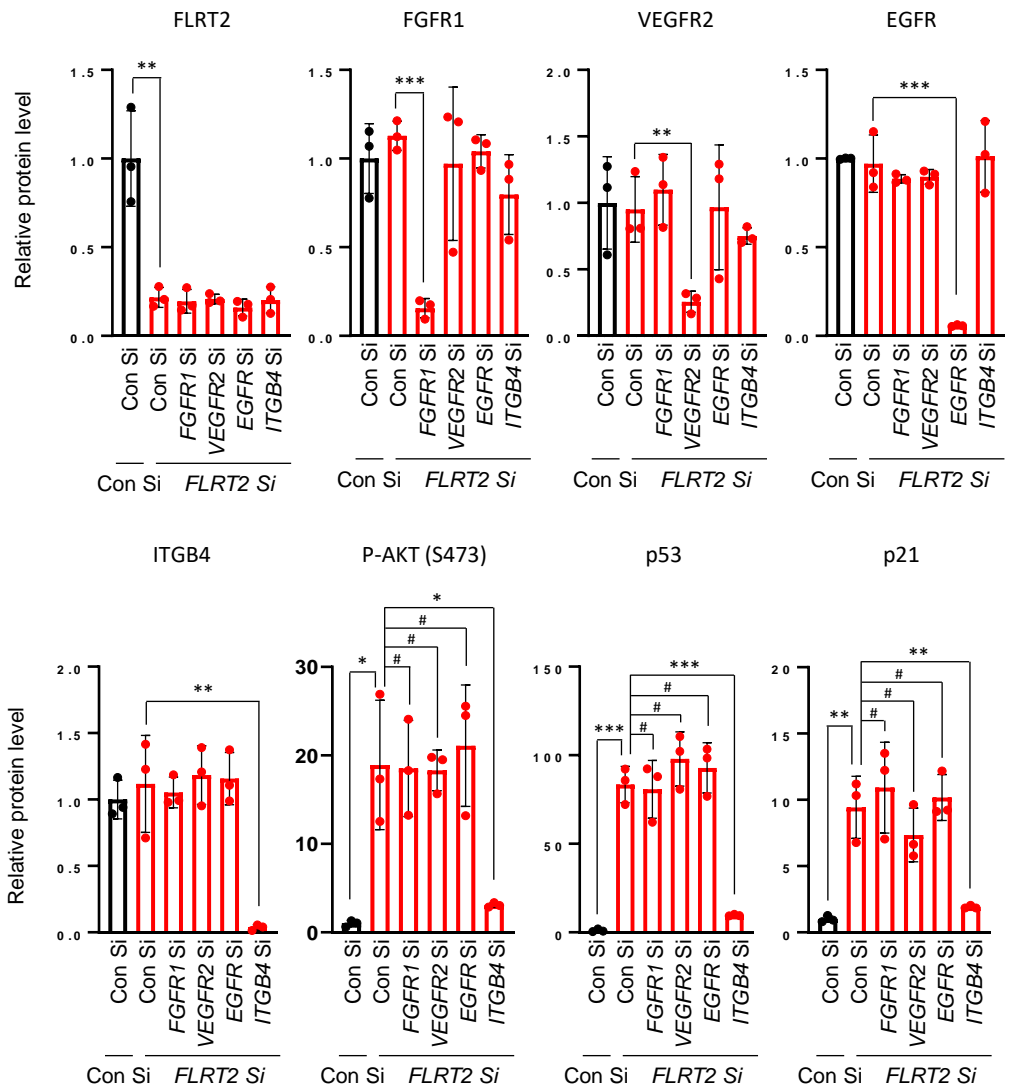
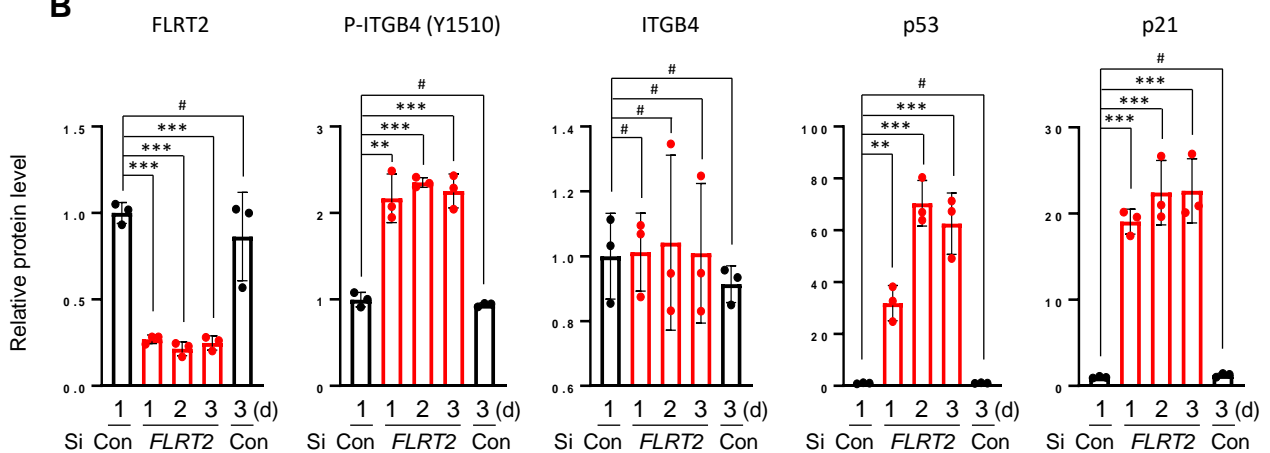
A**B**

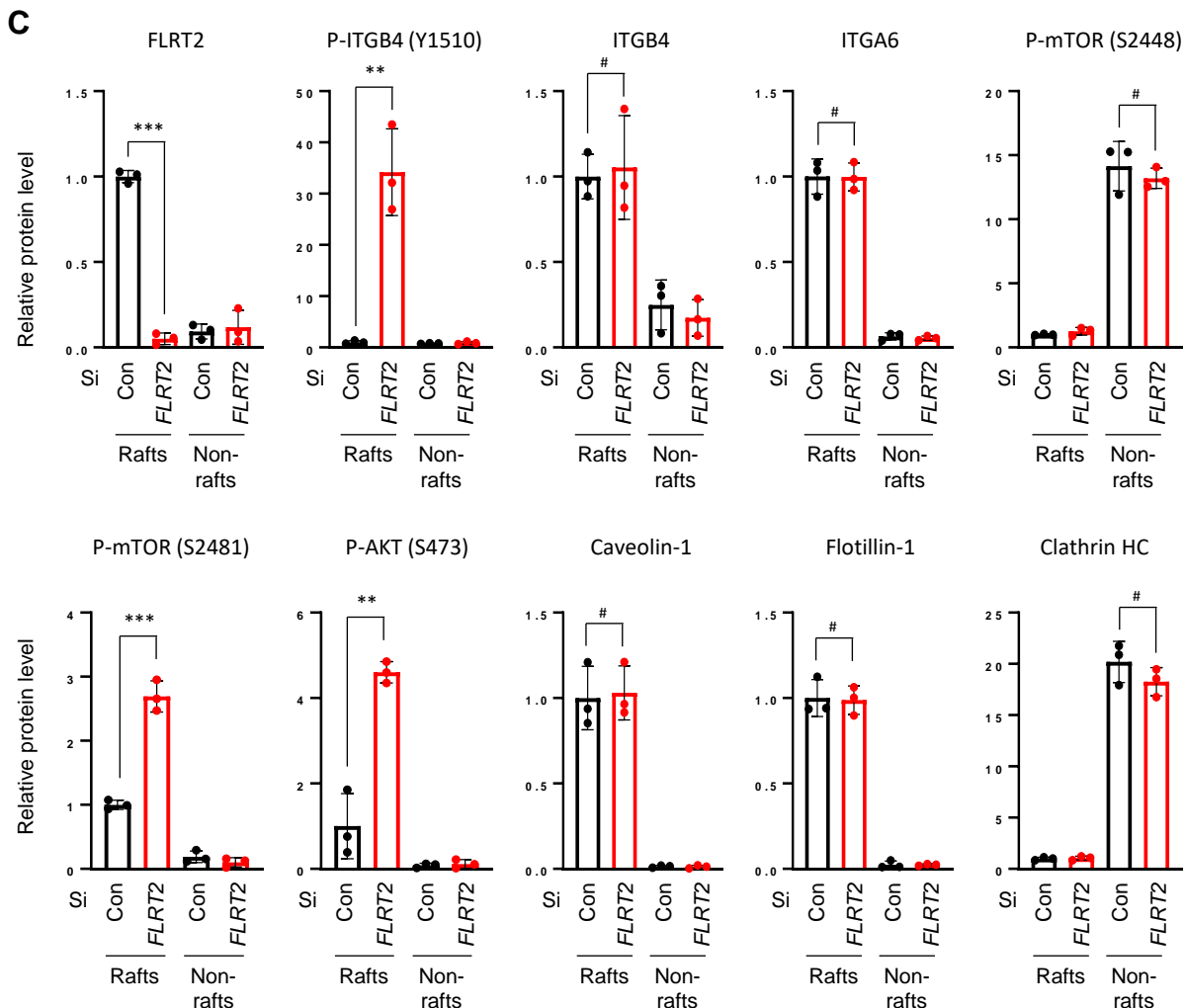
Candidates	Fold change
P-FGFR1 (Tyr766)	1.455
P-VEGFR2 (Tyr1059)	1.281
P-EGFR (Tyr1016)	1.23
P-ITGB4 (Tyr1510)	1.219

C**D**

Supplementary Figure 10. Analysis of protein phosphorylation changes in *FLRT2*-depleted HUVECs.

(A-B) The Phospho Explorer Antibody Array was used to screen total cell lysates from Con Si or *FLRT2* Si-transfected HUVECs cultures. The numbers of legends in the pie diagram indicate the fold change in protein phosphorylation of *FLRT2* Si-transfected cells, i.e. induced (green, orange), reduced (yellow), and unchanged (gray) **(A)**. The data shows the fold change of the indicated phosphoproteins 2 days after transfection with Con Si or *FLRT2* Si **(B)**. **(C)** HUVECs were transfected with Con Si or *FLRT2* Si, harvested at the indicated time points post-transfection, and subjected to immunoblotting. **(D)** HUVECs were transfected with Con Si, *Src* Si, or *AKT* Si (1st transfection) 6 h before transfection with Con Si or *FLRT2* Si (2nd transfection). At day 2 post-transfection, immunoblot assay was performed.

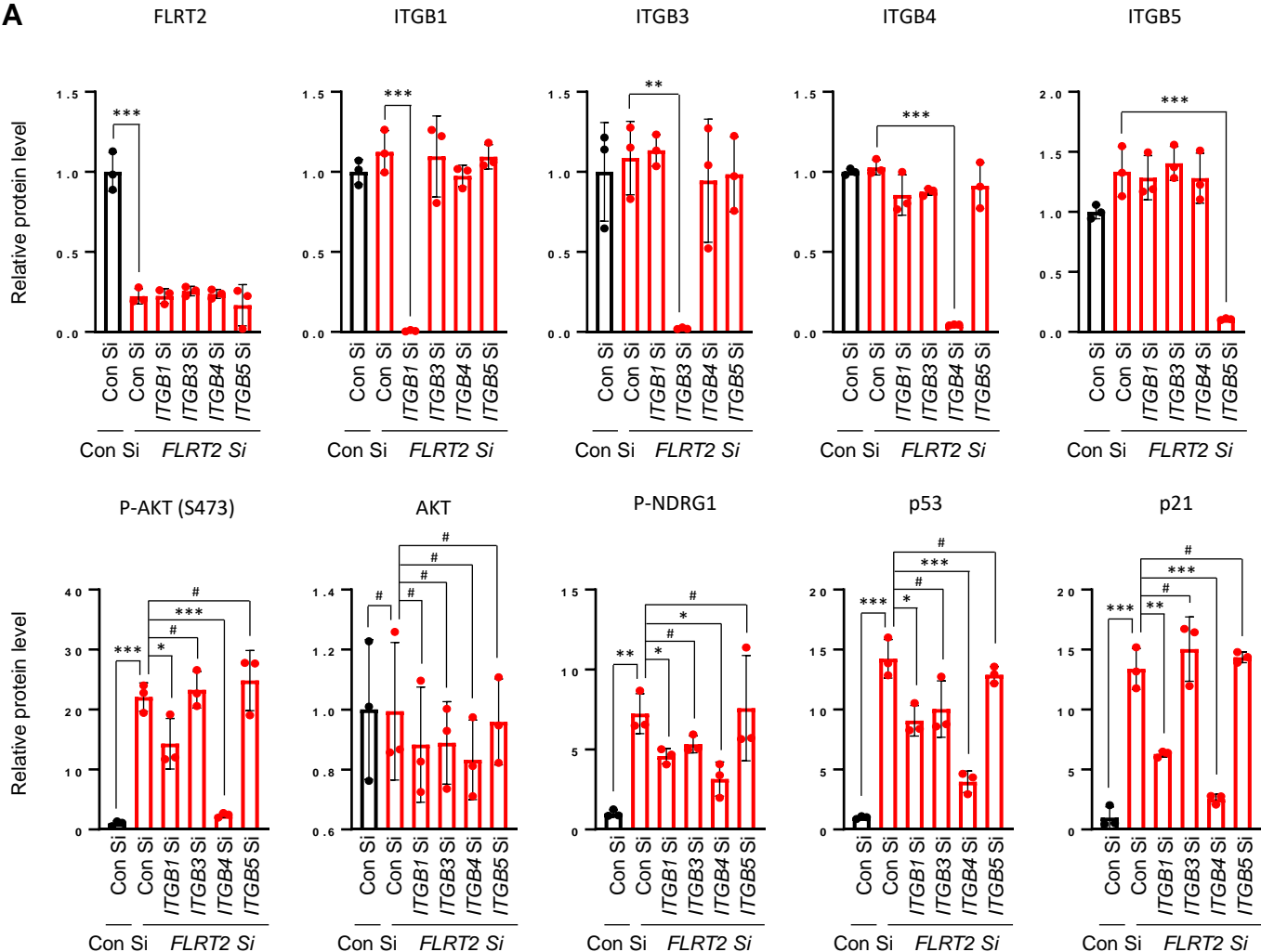
A**B**



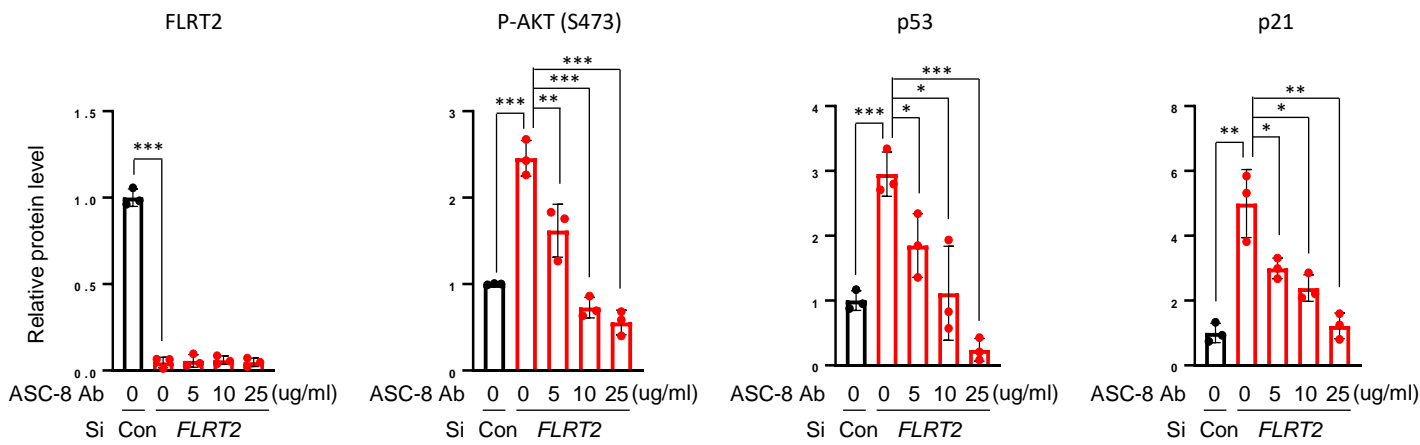
Supplementary Figure 11. Quantitative analysis of immunoblotting data presented in Fig. 3A, 3B, and 3G.

(A-C) The values represent mean \pm SD ($n = 3$; # $P > 0.05$; * $P < 0.05$; ** $P < 0.01$; *** $P < 0.001$).

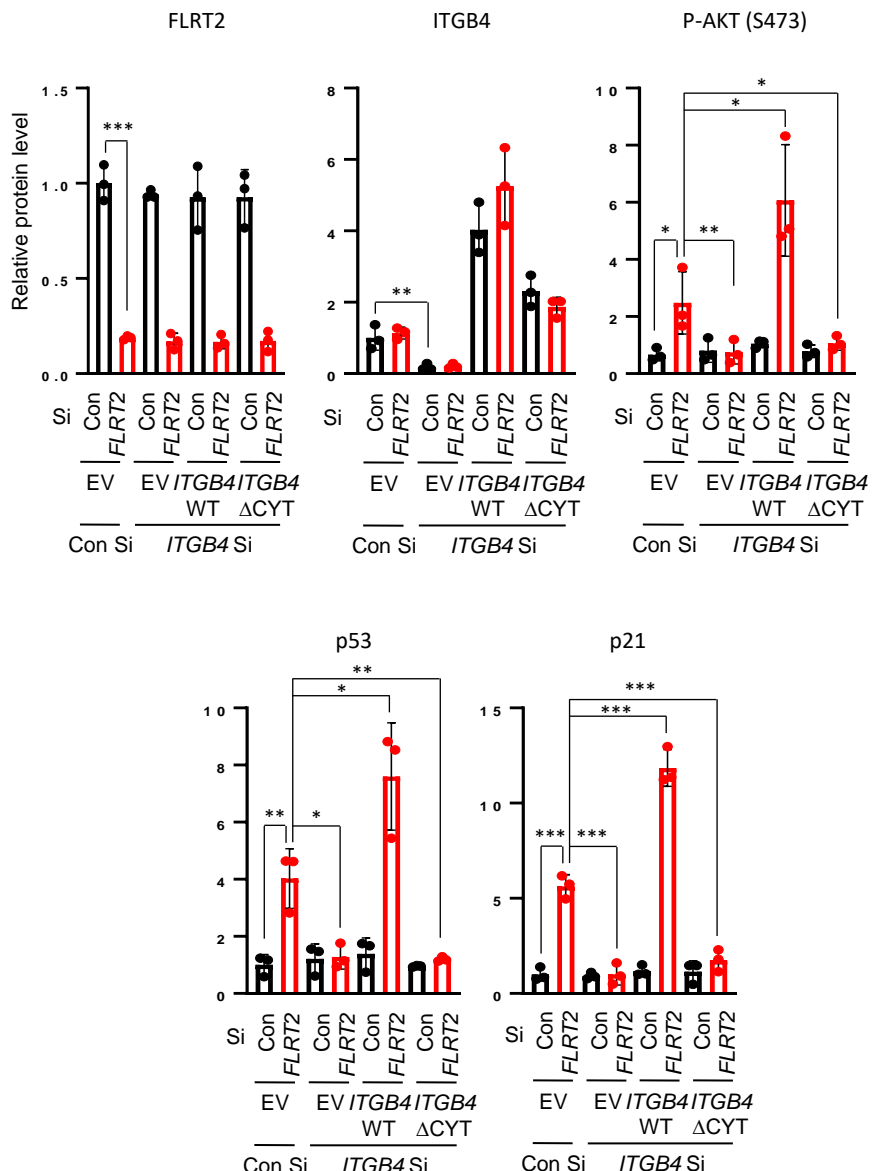
A



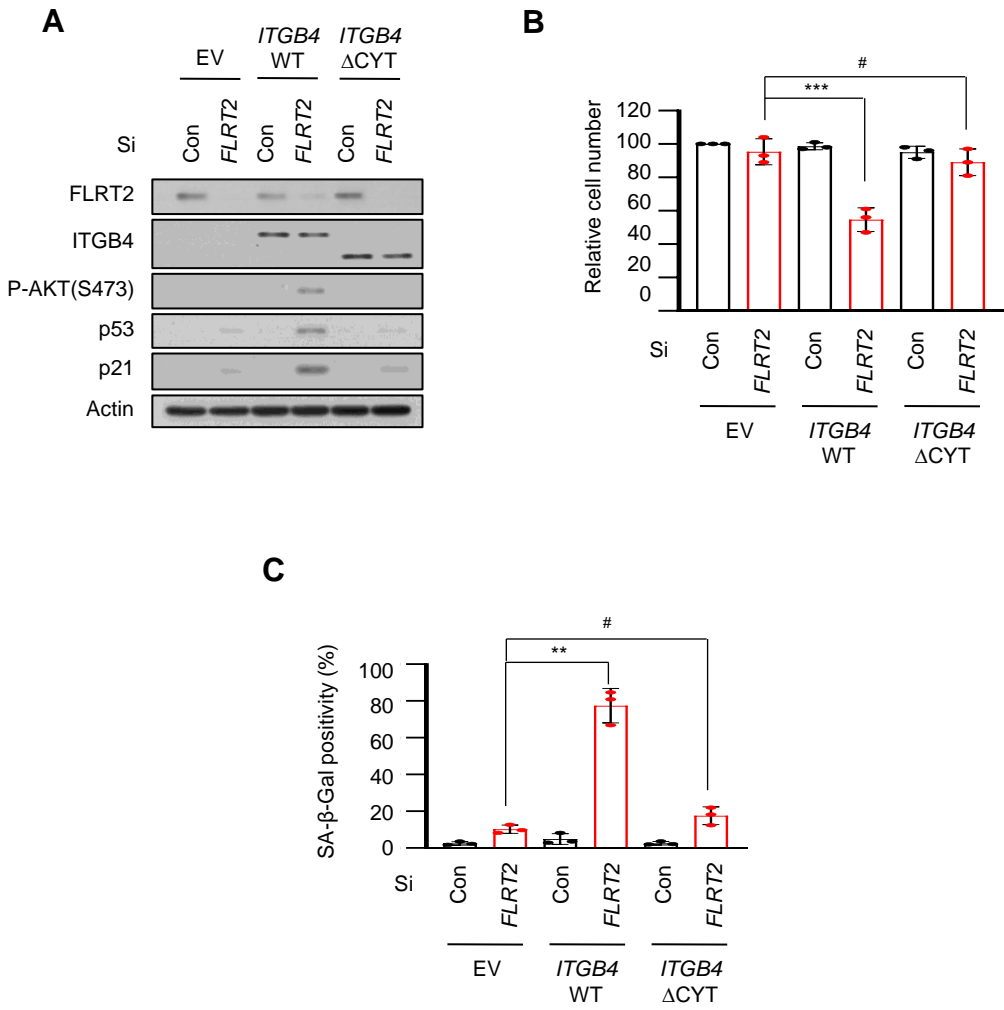
B



Supplementary Figure 12. Continued

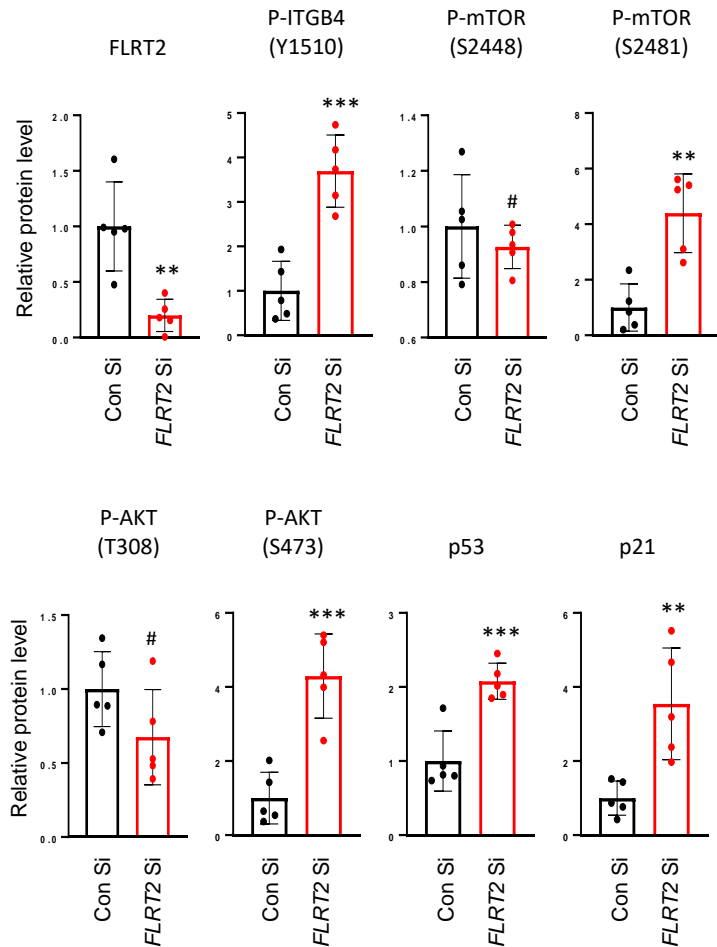
C

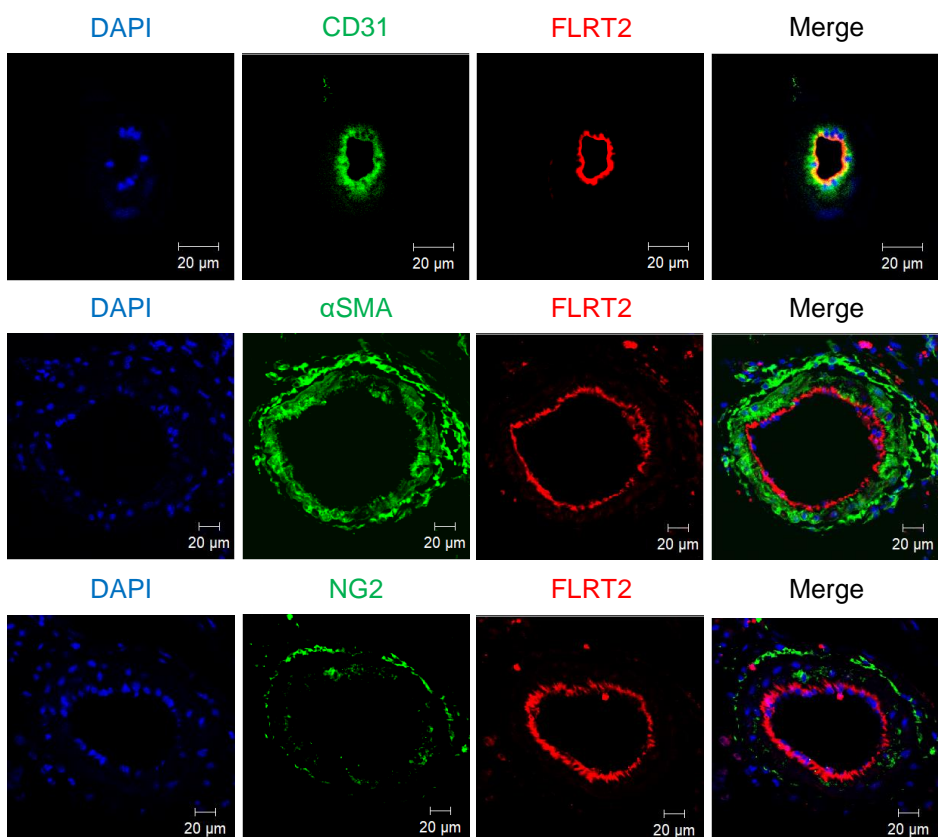
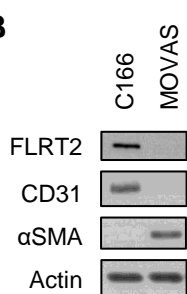
Supplementary Figure 12. Quantitative analysis of immunoblotting data presented in Fig. 4A, 4D and 4F.
(A-C) The values represent mean \pm SD ($n = 3$; # $P > 0.05$; * $P < 0.05$; ** $P < 0.01$; *** $P < 0.001$).



Supplementary Figure 13. The phosphorylation domain of integrin β 4 involves in *FLRT2* depletion-induced senescence in human aortic endothelial cells (HAECs).

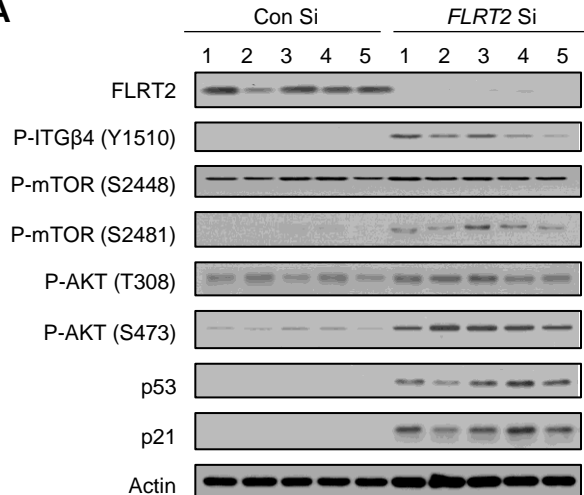
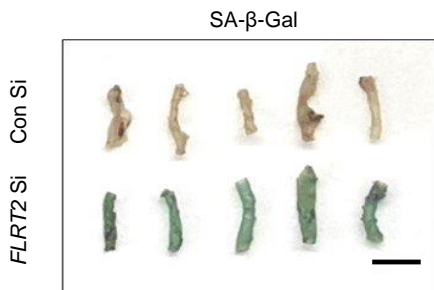
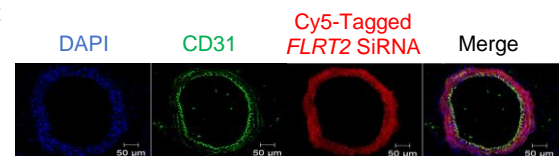
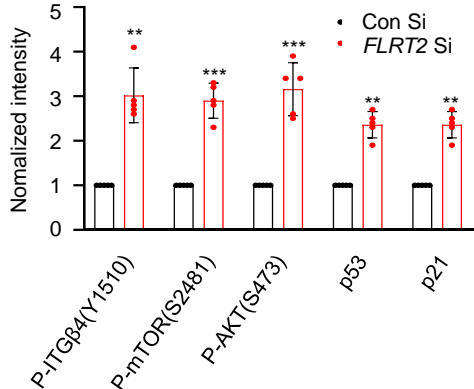
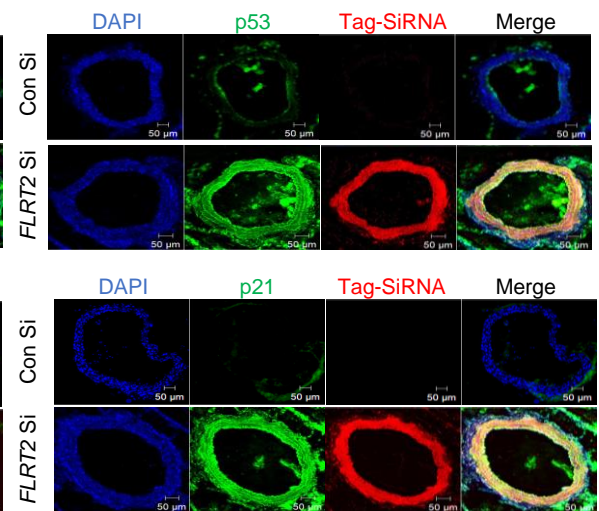
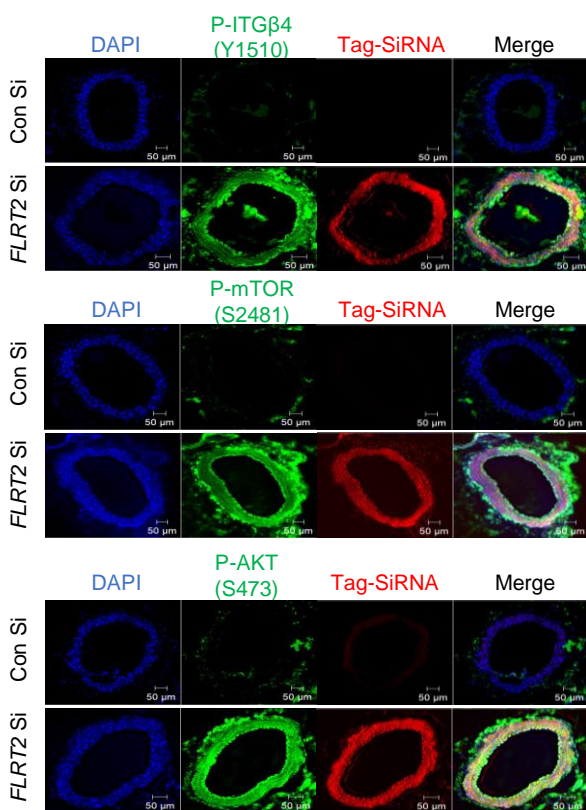
(A-C) Quantitative analysis of immunoblotting data presented in Fig. 4A, 4D and 4F. The values represent mean \pm SD (n = 3; #P > 0.05; *P < 0.05; **P < 0.01; ***P < 0.001). **(D-F)** HAEC were transfected with empty vector (EV) or a vector encoding wild-type *ITGB4* (WT) or a truncated mutant of *ITGB4* lacking the residues downstream of amino acid 1355 (Δ CYT), followed by transfection with Con Si or *FLRT2* Si. **(D)** Cell lysates were subjected to immunoblotting. Relative cell number **(E)** and SA- β -Gal activity **(F)** were measured at day 3 post-transfection. The values represent mean \pm SD (n = 3; #P > 0.05; **P < 0.01; ***P < 0.001).

A**Supplementary Figure 14. Quantitative analysis of immunoblotting data presented in Fig. 5A.**(A). The values represent mean \pm SD ($n = 3$; # $P > 0.05$; ** $P < 0.01$; *** $P < 0.001$).

A**B**

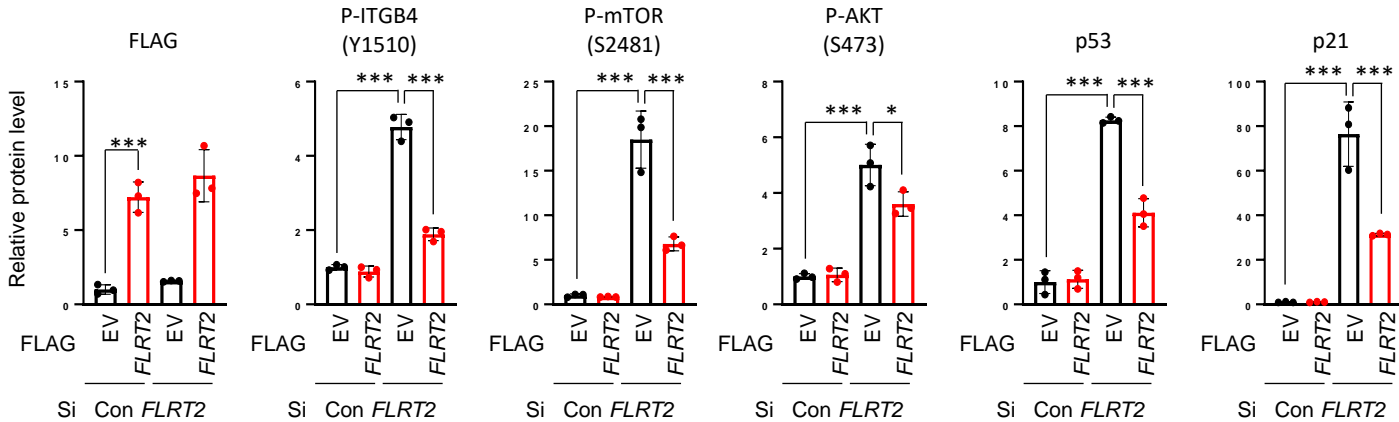
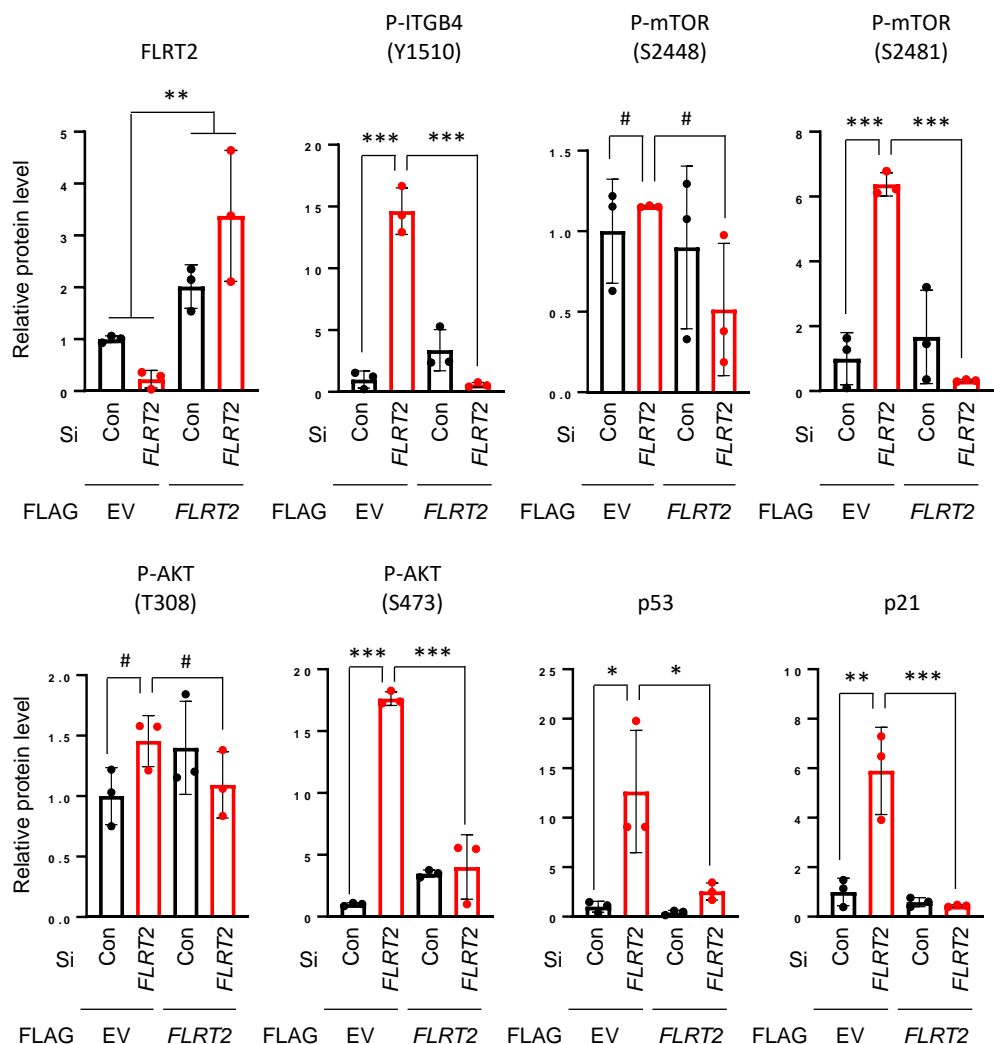
Supplementary Figure 15. Localization and expression of FLRT2 in mouse aorta and mouse cell lines.

(A) Representative images of immunofluorescence staining of CD31, α SMA, NG2, and FLRT2 in aortic cross sections of mice. (B) C166 and MOVAS cells were subjected to immunoblot assays with the indicated antibodies.

A**B****C****D**

Supplementary Figure 16. *In vivo* knockdown of *FLRT2* promotes cell senescence in veins of mice.

(A) Representative immunoblot images for venous lysates of mice injected intravenously with Con Si or *FLRT2* Si ($n = 5$). **(B)** Image of SA- β -Gal-stained veins of mice. Scale bar: 2 mm. **(C)** Fluorescence microscopies of venous cross sections obtained from mice injected intravenously with Cy5-tagged *FLRT2* Si. Nuclei are stained with DAPI (blue). Red and green signals show Cy5-tagged *FLRT2* Si and the endothelial marker, CD31, respectively. Merged image indicates siRNA uptake by the endothelium. **(D)** Immunostaining for P-ITGB4 (Y1510), P-mTOR (S2481), P-AKT (S473), p53, and p21 in veins of mice injected with the indicated siRNAs. The values represent mean \pm SD ($n = 5$; ** $P < 0.01$; *** $P < 0.001$).

A**B****Supplementary Figure 17. Quantitative analysis of immunoblotting data presented in Fig. 6A and 6D.****(A-B)**The values represent mean \pm SD ($n = 3$; # $P > 0.05$; * $P < 0.05$; ** $P < 0.01$; *** $P < 0.001$).